Synthesis and Characterization of Layered Silicate–Epoxy Nanocomposites

Phillip B. Messersmith† and Emmanuel P. Giannelis*

Department of Materials Science and Engineering, Cornell University, Ithaca, New York 14853

Received March 15, 1994. Revised Manuscript Received June 13, 1994®

An epoxy–silicate nanocomposite has been prepared by dispersing an organically modified mica-type silicate in an epoxy resin (diglycidyl ether of bisphenol-A, DGEBA) and curing in the presence of nadic methyl anhydride (NMA), benzyldimethylamine (BDMA), or boron trifluoride monoethylamine (BTFA) at 100–200 °C. Molecular dispersion of the layered silicate within the cross-linked epoxy matrix was verified using X-ray diffraction and transmission electron microscopy, revealing layer spacings of 100 Å or more and good wetting of the silicate surface by the epoxy matrix. The curing reaction appears to involve the hydroxyethyl groups of the alkylammonium ions located in the galleries of the organically modified silicate, which participate in the cross-linking reaction and result in direct attachment of the polymer network to the molecularly dispersed silicate layers. The nanocomposite exhibits a broadened T_g at slightly higher temperature than the unmodified epoxy. Furthermore, the dynamic storage modulus of the nanocomposite containing 4 vol % silicate was approximately 58% higher in the glassy region and 450% higher in the rubbery plateau region compared to the unmodified epoxy.

Introduction

Nanocomposites are a relatively new class of materials which exhibit ultrafine phase dimensions, typically in the range 1–100 nm.[1] Experimental work on these materials has generally shown that virtually all types and classes of nanocomposites lead to new and improved properties when compared to their micro- and macrocomposite counterparts.[1] We[2-8] as well as others[9-21] have investigated the design, synthesis, and characterization of polymer–ceramic nanocomposites. Our work, in particular, has centered on the use of mica-type silicates (MTS) for the formation of new polymer–ceramic nanocomposites with unique properties.[2-7]

MTSs belong to the general family of 2:1 layered silicates. Their structure consists of two fused silica tetrahedral sheets sandwiching an edge-shared octahedral sheet of either aluminum or magnesium hydroxide. Stacking of the layers leads to a regular van der Waals gap or interlayer.[22] Isomorphic substitution within the layers generates negative charges that are counterbalanced by cations residing in the interlayers. Although the natural forms of MTSs usually contain Na^+ or K^+ ions, ion-exchange reactions with organic cations (e.g., alkylammonium ions) can render the normally hydrophilic MTS organophilic.

While the number of nanocomposites based on MTSs and linear thermoplastics is growing,[11-14] little work has been devoted to cross-linked polymeric systems such as epoxies.[10] Recent reports of particulate-based epoxy composites suggest that the dimensional stability, conductivity, mechanical, thermal, and other properties may be modified due to the incorporation of filler particles within the epoxy matrix.[23-30] For the most part, however, the improvements in properties observed with these conventionally prepared composites are modest when compared (on an equal volume basis of particulate filler) to those that have been established for various polymer–ceramic nanocomposites.

Previous work on poly(amide),[11-13] poly(imide),[14] and our ongoing experiments with poly(ϵ-caprolactone)[2,4] has demonstrated the feasibility of dispersing molecular

† Current address: Department of Restorative Dentistry, University of Illinois at Chicago, Chicago, IL 60612.

® Abstract published in *Advance ACS Abstracts,* July 15, 1994.

(1) For a recent review of nanocomposites, see: Komarneni, S. *J. Mater. Chem.* **1992**, *2*, 1219.
(2) Messersmith, P. B.; Giannelis, E. P. *Chem. Mater.* **1993**, *5*, 1064.
(3) Vaia, R. A.; Ishii, H.; Giannelis, E. P. *Chem. Mater.* **1993**, *5*, 1694.
(4) Messersmith, P. B.; Giannelis, E. P., submitted for publication.
(5) Mehrotra, V.; Giannelis, E. P. *Solid State Ionics* **1992**, *51*, 115.
(6) Mehrotra, V.; Giannelis, E. P. *Solid State Commun.* **1991**, *77*, 155.
(7) Mehrotra, V.; Keddie, J. L.; Miller, J. M.; Giannelis, E. P. *J. Non-Crystalline Solids* **1991**, *136*, 97.
(8) Ziolo, R. F.; Giannelis, E. P.; et al. *Science* **1992**, *257*, 219.
(9) Messersmith, P. B.; Stupp, S. I. *J. Mater. Res.* **1992**, *7*, 2599.
(10) Wang, M. S.; Pinnavaia, T. J., submitted for publication.
(11) Usuki, A.; et al. *J. Mater. Res.* **1993**, *8*, 1179.
(12) Okada, A.; Kawasumi, M.; Usuki, A.; Kojima, Y.; Kurauchi, T.; Kamigaito, O. *Mater. Res. Soc. Symp. Proc.* **1990**, *171*, 45.
(13) Okada, A.; Kawasumi, M.; Kurauchi, T.; Kamigaito, O. *Polym. Prepr.* **1987**, *28*, 447.
(14) Yano, K.; et al. *J. Polym. Sci., Part A: Polym. Chem.* **1993**, *31*, 2493.
(15) Coltrain, B. K.; et al. *Chem. Mater.* **1993**, *5*, 1445.
(16) Huang, H. H.; Orler, B.; Wilkes, G. L. *Macromolecules* **1987**, *20*, 1322.
(17) Wang, S.; Ahmad, Z.; Mark, J. E. *Polym. Bull.* **1993**, *31*, 323.
(18) Novak, B. M. *Adv. Mater.* **1993**, *5*, 422.
(19) Saegusa, T. *Polym. Prepr.* **1993**, *34*, 804.
(20) Wei, Y.; Dachung, Y.; Tang, L.; Hutchins, M. K. *J. Mater. Res.* **1993**, *8*, 1143.
(21) Nandi, M.; Conklin, J. A.; Salvati, L., Jr.; Sen, A. *Chem. Mater.* **1991**, *3*, 201.
(22) Grim, R. E. *Clay Mineralogy*; McGraw-Hill: New York, 1953.
(23) Nakamura, Y.; Yamaguchi, M.; Tanaka, A.; Okubo, M. *Polymer* **1993**, *34*, 3220.
(24) Koh, S. W.; Kim, J. K.; Mai, Y. W. *Polymer* **1993**, *34*, 3446.
(25) Papanicolaou, G. C.; Bakos, D. *J. Reinf. Plast. Compos.* **1992**, *11*, 104.
(26) Paipetis, S. A.; Papanicolaou, G. C.; Theocaris, P. S. *Fibre Sci. Technol.* **1975**, *8*, 221.
(27) Amdouni, N.; Sautereau, H.; Gerard, J. F. *J. Appl. Polym. Sci.* **1992**, *45*, 1799.
(28) Ding, J.; Chen, C.; Xue, G. *J. Appl. Polym. Sci.* **1991**, *42*, 1459.
(29) Inubishi, S.; et al. *J. Mater. Sci.* **1988**, *23*, 1182.
(30) Petrovic, Z.; Stojakovic, N. *Polym. Composites* **1988**, *9*, 42.

0897-4756/94/2806-1719$04.50/0

silicate layers within a macromolecular matrix which results in significant improvements in physical properties with only modest particulate contents (<10% by volume). Similarly, our goal is to synthesize a polymer–ceramic nanocomposite in which MTS individual layers with a thickness 10 Å and a high aspect ratio (100–1000) are dispersed within a cross-linked epoxy matrix.

Wang and Pinnavaia[10] have recently reported delamination of MTS in an epoxy resin by heating an onium ion exchanged form of montmorillonite with epoxy resin to temperatures of 200–300 °C. X-ray and electron microscopy studies of the composite suggested delamination of the silicate layers, although phase segregation of the polyether-coated MTS from the epoxy matrix was observed. Furthermore, the product of the high-temperature curing reaction is an intractable powder rather than a continuous solid epoxy matrix. Thus, a great need still exists for the development of an MTS–epoxy nanocomposite which can be mixed, applied in various forms (e.g., as adhesive films, coatings, or castings), and cured by conventional means. We report here on the preparation of an MTS–epoxy nanocomposite which fulfills these requirements and is processed using conventional epoxy curing agents at temperatures significantly lower than those previously reported.[10] The resulting composite exhibits molecular dispersion of the silicate layers in the epoxy matrix, good optical clarity, and significantly improved dynamic mechanical properties compared to the unmodified epoxy.

Experimental Section

Synthesis of Nanocomposite. An organically modified mica-type silicate (OMTS, supplied by Southern Clay Products, Gonzales, TX) was prepared by an ion-exchange reaction from Na–montmorillonite and bis(2-hydroxyethyl) methyl tallow–alkyl ammonium chloride (Ethoquad T/12, Akzo Chemicals) as shown in eq 1, where R′ is predominantly an octadecyl chain

$$Na^+\text{–MTS} + (HOCH_2CH_2)_2R'R''N^+Cl^- \rightarrow (HOCH_2CH_2)_2R'R''N^+\text{–MTS} + NaCl \quad (1)$$

with smaller amounts of lower homologues (approximate composition: C_{18} 70%, C_{16} 25%, C_{14} 4%, and C_{12} 1%) and R″ is a methyl group. The dry OMTS powder was added with stirring to diglycidyl ether of bisphenol A (DGEBA, Dow Chemical's *DER 332*, epoxide equivalent weight = 178) and cured by addition of either nadic methyl anhydride (NMA, Aldrich), boron trifluoride monoethylamine (BTFA, Aldrich), benzyldimethylamine (BDMA, Aldrich), or methylenedianiline (MDA, Aldrich). The amount of curing agent used for each formulation was as follows: DGEBA/NMA: 87.5 parts of NMA/hundred resin (phr), with or without 1.5 phr BDMA. DGEBA/BDMA: 1.5–10 phr BDMA. DGEBA/BTFA: 3 phr BTFA. DGEBA/MDA: 27 phr MDA. OMTS/DGEBA mixtures were held at 90 °C with stirring for 1 h and then sonicated for 1–2 min while hot using a Fisher Model 300 Sonic Dismembrator (Fisher Scientific, Itasca, IL). Following sonication samples were cooled, curing agent was added with thorough mixing, and then loaded into disposable syringes. Samples were centrifuged in the syringes for 30 s at 3000 rpm to remove bubbles, and then dispensed into rectangular teflon molds with dimensions 20 mm by 10 mm by 1.5 mm thick, or casted as free-standing films with thicknesses of 0.1–0.3 mm. All samples were cured at 100 °C for 4 h, 150 °C for 16 h, and 200 °C for 12 h (in vacuo).

Characterization of Nanocomposite. X-ray diffraction (XRD) experiments were performed directly on the nanocomposite samples using a Scintag Pad X diffractometer with Cu (λ = 1.54 Å) or Cr (λ = 2.29 Å) irradiation. In situ, hot-stage XRD experiments were conducted using a special thermal attachment which allowed samples to be heated to a number of different temperatures without removing the sample from the diffractometer. Samples were ramped at 10 °C/min between the set temperatures, and scanned after a 10 min isothermal equilibration. The exothermic epoxy curing reaction was followed by differential scanning calorimetry (DSC) using a duPont 9900 thermal analyzer. Spectra were obtained under flowing nitrogen at a scanning rate of 10 °C/min. In situ infrared curing studies were performed on a Mattson Galaxy 2020 Series FT-IR using a programmable variable temperature heating cell (Model HT-32, Spectra-Tech, Inc.). Spectra were collected at a resolution of 4 cm^{-1}. Composite microstructure was imaged using transmission electron microscopy (TEM) on carbon-coated 100 nm thick sections of the composite using a JEOL 1200EX transmission electron microscope at an accelerating voltage of 120 kV. Dynamic mechanical analyses (DMA) of the cured composite films were performed on a Rheovibron DDV-II-C viscoelastometer (Toyo Baldwin Co., Japan) operating at a driving frequency of 110 Hz and a temperature scanning rate of 1 °C/min.

Results and Discussion

Nanocomposite Synthesis. The synthetic procedure used for nanocomposite preparation is essentially that initially developed by Usuki et al. for nylon–silicate nanocomposites.[11–13] In its most basic form it involves dispersion of the organically modified mica-type silicate (OMTS) in a suitable monomer, followed by polymerization. Under proper conditions delamination of the OMTS into individual silicate layers occurs, which ultimately become dispersed within the macromolecular matrix. We used a similar synthetic protocol which involved mixing of OMTS and DGEBA at 90 °C, followed by sonication, addition of curing agent, and curing of the network at a prescribed set of temperatures.

Initial mixing of OMTS and DGEBA was performed at 90 °C to ensure low resin viscosity. Following addition of small amounts of OMTS (10% by weight or less) the resin viscosity was only slightly increased. However, samples sonicated briefly (1–2 min) experienced a significant increase in resin viscosity at relatively low shear rates while turning from opaque to semitransparent during sonication. OMTS loadings of 10% (w/w) or more resulted in strong gel formation during sonication, even after reheating to temperatures at or above 100 °C. We suggest that the observed increase in resin viscosity following sonication is due to the dispersion of high aspect ratio (100–1000) silicate layers within the epoxy resin and is due to formation of a so-called "house of cards" structure, in which edge-to-edge and edge-to-face interactions between dispersed layers form percolation structures. Similar rheological changes have been observed when OMTSs are dispersed in various organic media and attributed to the formation of the "house-of cards" structure.[31–33]

Delamination of OMTS. XRD analysis was used to follow the progress of OMTS dispersion during mixing with DGEBA and subsequent curing reactions. Figure 1 shows XRD patterns of dry OMTS and the uncured OMTS/DGEBA mixture. The XRD pattern of the OMTS powder shows a primary silicate (001) reflection at 2Θ = 4.8°, with a low-intensity shoulder at roughly 2Θ =

(31) Granquist, W. T.; McAtee, J. L. *J. Colloid Sci.* **1963**, *18*, 409–420.
(32) Damerell, V. R.; Milberger, E. C. *Nature* **1956**, *178*, 200.
(33) Kemnetz, S. J.; Still, A. L.; Cody, C. A.; Schwindt, R. *J. Coatings Technol.* **1989**, *61*, 47–55.

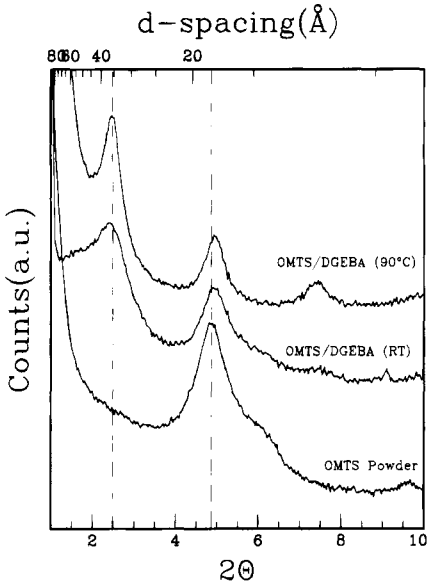

Figure 1. XRD patterns of OMTS powder and uncured OMTS/DGEBA mixture. Top scan was obtained at room temperature following heating of OMTS/DGEBA mixture at 90 °C for 1 h.

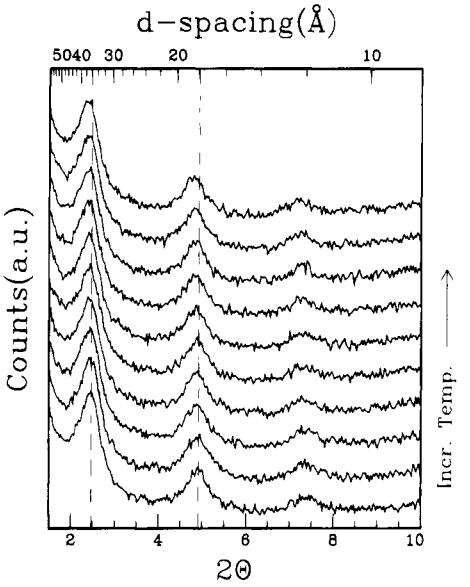

Figure 2. XRD patterns of OMTS/DGEBA mixture (4% MTS by volume) heated in situ to various temperatures. The spectra are displaced vertically for clarity, with scan temperatures (°C) from bottom to top as follows: 20; 50; 70, 90; 100; 110; 120; 130; 140; 150. The dashed lines indicate the location of the silicate (001) and (002) reflections at 20 °C.

5.8°. The main silicate reflection in OMTS corresponds to a layer d spacing of 17 Å which represents an increase of approximately 7 Å from the van der Waals gap of Na–montmorillonite.[22] Following mixing of OMTS and DGEBA at room temperature, an additional reflection centered at $2\Theta = 2.5°$ emerges which corresponds to intercalated OMTS/DGEBA. As is widely known, OMTS can readily intercalate various small organic molecules from either the vapor or liquid phase.[2,5,6,34–38] The second peak at $2\Theta = 5°$ corresponds to the coexistence of unintercalated ($d_{(001)} = 17$ Å) and intercalated ($d_{(002)} = 17.5$ Å) OMTS. The persistence of some unintercalated OMTS at room temperature can also be seen by the small remnant shoulder at $2\Theta = 5.8°$. In contrast, mixing of DGEBA and OMTS at 90 °C results in only DGEBA intercalated OMTS ($d_{(001)} = 35$ Å) with no residual OMTS peaks observed, as shown in the top trace of Figure 1. The reflections observed at $2\Theta = 2.5°$, 4.9°, and 7.6° correspond to the (001), (002), and (003) reflections of the DGEBA intercalated phase, respectively. Further evidence for the presence of only intercalated OMTS/DGEBA comes from the disappearance of the OMTS shoulder at $2\Theta = 5.8°$, which is no longer masked by any of the silicate (00l) reflections.

The XRD results discussed above relate to resin samples cooled to room temperature after mixing at 90 °C and, therefore, do not necessarily represent the structures present at the mixing and curing temperatures. Dynamic high-temperature, in situ XRD experiments were used to determine the exact structure of the resin mixtures at elevated temperatures. Samples were prepared by mixing OMTS and DGEBA in a vial at 90 °C, and cooling to room temperature before transferring to the diffractometer chamber. Shown in Figure 2 are a series of XRD scans of the OMTS/DGEBA mixture previously heated to 90 °C taken at various intervals between room temperature and 150 °C. The low temperature scans exhibit 3 orders of reflections indicating the existence of DGEBA intercalated OMTS with $d_{(001)} = 36$ Å. With increasing temperature a gradual increase in $d_{(001)}$ from 36 Å to approximately 38 Å was observed, although the constant intensity of the peaks suggests that little or no delamination occurs at or below 150 °C.

With the observation that intercalation but not delamination of OMTS occurs in the presence of DGEBA, we set out to identify potential epoxy curing agents which would produce both delamination of OMTS and crosslinking of the epoxy resin. Early on, it was observed that the choice of curing agent was critical in determining delamination and optical clarity. A survey of common epoxy curing agents revealed an unexpected obstacle: many curing agents studied resulted in little or no increase in layer separation, resulting in composites with silicate d-spacings of 30–40 Å or less. An example of this behavior is shown in Figure 3 for methylenedianiline (MDA) cured OMTS/DGEBA composite. This composite was prepared by adding MDA to the OMTS/DGEBA mixture, which resulted in immediate clouding of the resin. Interestingly, all bifunctional primary and secondary amine curing agents used were found to have this effect and resulted in opaque composites, in contrast to the transparent composites following delamination of OMTS. One possibility for this behavior might be the bridging of the silicate layers by the bifunctional amine molecules, which prevents further expansion of the layers. Another possibility is that the N–H groups in the primary and secondary amines are sufficiently polar to cause reaggregation of dispersed silicate layers. Others have observed similar degellation (deexfoliation) of OMTSs dispersed in organic solvents upon the addition of polar additives.[33]

(34) Theng, B. K. G. *The Chemistry of Clay-Organic Reactions*; Adam Hilger, Ltd.: London, 1974.
(35) Kanatzidis, M. G.; Wu, C. *J. Am. Chem. Soc.* **1989**, *111*, 4139.
(36) Pillion, J. E.; Thompson, M. E. *Chem Mater.* **1991**, *2*, 222.
(37) Divigalpitiya, W. M. R.; Frindt, R. F.; Morrison, S. R. *J. Mater. Res.* **1991**, *6*, 1103.
(38) Blumstein, A. *J. Polym. Sci., Part A* **1965**, *3*, 2653.

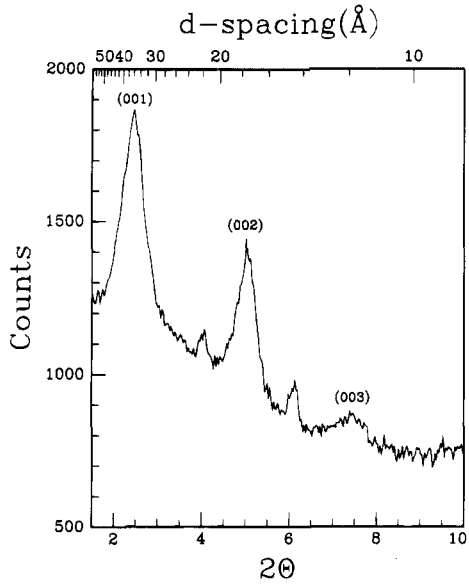

Figure 3. XRD pattern of fully cured OMTS/DGEBA/MDA composite containing 2% OMTS by volume. The silicate (001) reflection corresponds to a layer spacing of 36 Å. The weak reflections at $2\Theta = 4.1°$ and 6.1° most likely correspond to MDA intercalated OMTS and unintercalated OMTS, respectively.

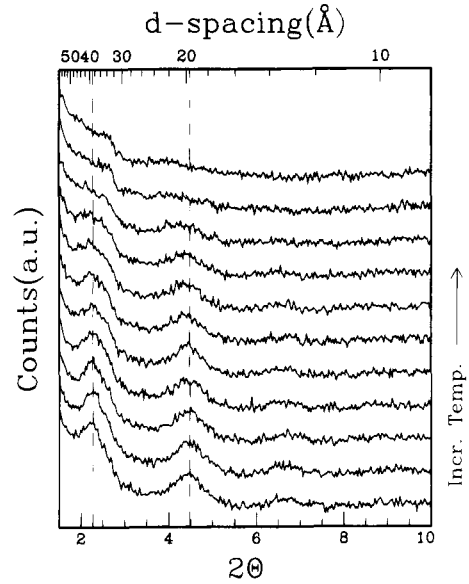

Figure 4. XRD patterns of OMTS/DGEBA/BDMA mixture (4% MTS by volume) heated in situ to various temperatures. The spectra are displaced vertically for clarity, with scan temperatures (°C) from bottom to top as follows: 20; 40; 50; 60, 70; 80; 90; 100; 110; 130; 150. The dashed lines indicate the location of the silicate (001) and (002) reflections at 20 °C.

Unlike the primary and secondary amines, a number of curing agents (NMA, BDMA, BTFA, and combinations thereof), were found to result in OMTS delamination during heating of the reaction mixture. Shown in Figure 4 are in situ XRD scans of the OMTS/DGEBA/BDMA mixture illustrating the delamination of OMTS on heating from room temperature to 150 °C. As before, the sample was prepared by mixing OMTS and DGEBA in a vial at 90 °C, cooling to room temperature, and mixing in BDMA immediately before transferring to the diffractometer chamber. The mixing of BDMA into the OMTS/DGEBA resin at room temperature resulted in an intercalated system with $d_{(001)} = 39$ Å (slightly

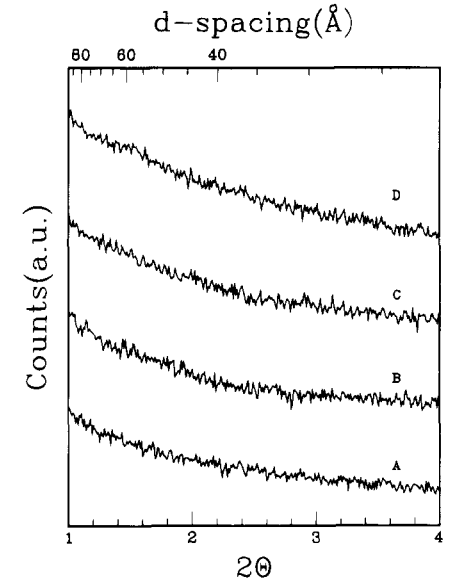

Figure 5. XRD patterns of fully cured OMTS/DGEBA/BDMA nanocomposites containing A: 0.4% B: 1.2% C: 2% D: 4% OMTS by volume. Spectra are displaced vertically for clarity.

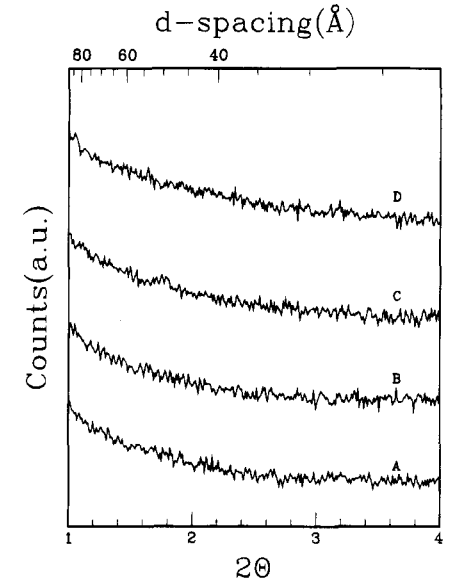

Figure 6. XRD patterns of fully cured OMTS/DGEBA/NMA nanocomposites containing A: 0.4% B: 1.2% C: 2% D: 2.8% OMTS by volume. Spectra are displaced vertically for clarity.

expanded from the $d_{(001)} = 36$ Å observed with OMTS/DGEBA). Furthermore, in contrast to what we observed in the absence of a curing agent heating of the OMTS/DGEBA/BDMA mixture resulted in substantial attenuation of the peak at $2\Theta = 2.3°$. This peak almost disappeared by 150 °C (top of Figure 4), with only a trace remaining at $2\Theta = 3°$. The virtual disappearance of the OMTS (001) reflections clearly indicates delamination of OMTS has taken place.

XRD analysis of completely cured nanocomposite samples also lacked silicate (00l) reflections as shown in Figures 5 and 6 for OMTS/DGEBA/BDMA and OMTS/DGEBA/NMA, respectively. The absence of silicate (00l) reflections in the cured nanocomposites shows that the delamination and dispersion of the silicate layers within the epoxy matrix is retained after complete curing of the epoxy. The exfoliation of the silicate was further confirmed using TEM. The micrographs

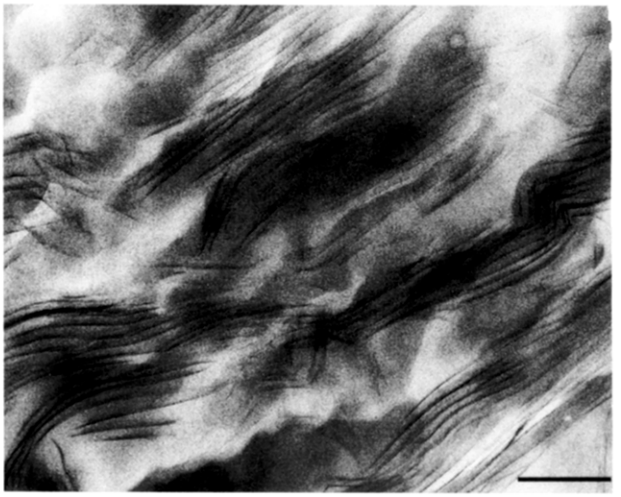

A

B

Figure 7. TEM micrographs of thin sections of fully cured OMTS/DGEBA/NMA nanocomposite containing 4% MTS by volume. Dispersed silicate layers are viewed edge-on and are clearly visible as dark lines of thickness approximately 10 Å, with 80–120 Å of epoxy matrix separating neighboring silicate layers. Scale bars = (a) 100 nm and (b) 10 nm.

of the BDMA-cured composite are shown in Figure 7. These micrographs show quite clearly the existence of well-dispersed individual silicate layers (dark lines in Figure 7) of thickness 1 nm embedded in the epoxy matrix. Some areas of the epoxy matrix appear to contain oriented collections of 5–10 parallel silicate layers. These domains of parallel layers are presumably remnants of OMTS tactoids, but with substantial expansion of the gallery beyond that corresponding to an intercalated silicate phase (see, for example, Figures 1 and 3). Close examination of these domains reveals consistent layer spacings of approximately 100 Å or more, with the intervening galleries between layers filled with crosslinked epoxy matrix. It is particularly interesting to note that the samples are mostly homogeneous with no phase separation between the silicate layers and the epoxy matrix. In fact, examination of the micrographs shows excellent apposition between the MTS layers and the polymeric matrix.

Curing Reactions. In contrast to the work of Wang and Pinnavaia,[10] where no curing agent was added, we use a curing agent that either cross-links DGEBA in the presence of OMTS, reacts directly with OMTS, or catalyzes the cross-linking reaction between OMTS and DGEBA.[39–42] The benefits of this approach are first, curing of the nanocomposite occurs at much lower temperatures than reported previously,[10] and second, formation of chemical bonds between the cross-linked network and the silicate nanoparticles results in direct attachment of the epoxy matrix to the silicate layers, thereby maximizing interfacial adhesion between the two phases.

A particularly interesting case is that of the curing agent BDMA, which can catalyze the homopolymerization of DGEBA, but is also capable of catalyzing the reaction between hydroxyl groups of the alkylammonium ions and the oxirane rings of DGEBA.[39,40] Our experiments indicate that curing conditions of the composite resin may have an affect on the reaction mechanism. For example, increasing the temperature of the OMTS/DGEBA/BDMA and DGEBA/BDMA mixtures from 20 to 250 °C at slow rates (0.5 °C/min) resulted in little difference in curing behavior between the composite and unmodified epoxy as shown by comparing the corresponding infrared spectra (Figure 8). Both series of spectra show a gradual disappearance of the epoxy band at 918 cm^{-1} at temperatures between 80 and 150 °C. The extent of DGEBA reaction as given by the intensity of the epoxy peak is roughly equivalent for both compositions (OMTS/DGEBA/BDMA and DGEBA/BDMA).

At higher heating rates, however, a difference in curing behavior is seen. Figure 9 shows DSC scans of the OMTS/DGEBA/BDMA and DGEBA/BDMA curing reactions at a scanning rate of 10 °C/min, showing a strong exotherm associated with curing between 100 and 150 °C for OMTS/DGEBA/BDMA. That the DSC scan of the DGEBA/BDMA mixture shows a considerably smaller exotherm over the same temperature range suggests OMTS plays a catalytic role in the base-catalyzed homopolymerization of DGEBA, or that the reaction proceeds by an altogether different mechanism in the presence of OMTS. One possibility as shown in eq 2 involves the base-catalyzed oxirane ring-opening

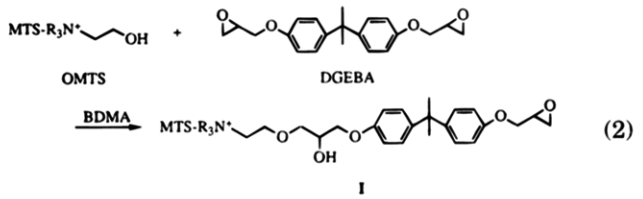

(2)

reaction between hydroxyl groups of OMTS and DGEBA resulting in formation of **I**, an OMTS–glycidyl ether of bisphenol A oligomer. **I** can subsequently react with free DGEBA via similar base-catalyzed oxirane ring

(39) Tanaka, Y.; Bauer, R. S. In *Epoxy Resins*; May, C. A., Ed.; Marcel Dekker: New York, 1988; p 285.
(40) Tanzer, W.; Reinhardt, S.; Fedtke, M. *Polymer* **1993**, *34*, 3520.
(41) Tanaka, Y.; Kakiuchi, H. *J. Appl. Polym. Sci.* **1963**, *7*, 1063.
(42) Lee, L.-H.; Pankey, J. W.; Heeschen, J. P. *J. Polym. Sci., Part A* **1965**, *3*, 2955.
(43) Sample contained 10% by weight OMTS. TGA analysis of OMTS indicated total organic content to be 20%. Taking into account the difference in density between mica-type silicates and cured epoxies, the silicate content was calculated to be 4% by volume.

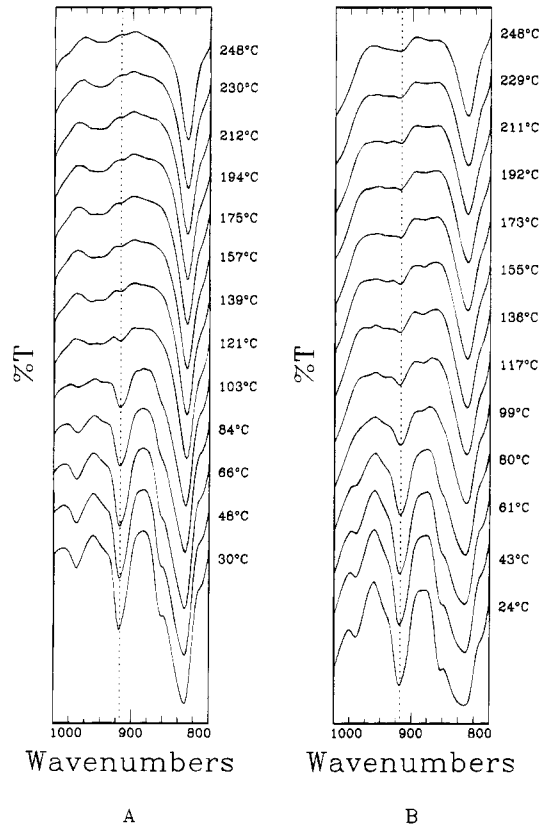

Figure 8. FT-IR spectra of (A) DGEBA/BDMA and (B) OMTS/DGEBA/BDMA (4 vol % MTS) resin mixtures taken at various temperatures during heating in situ at 0.5 °C/min.

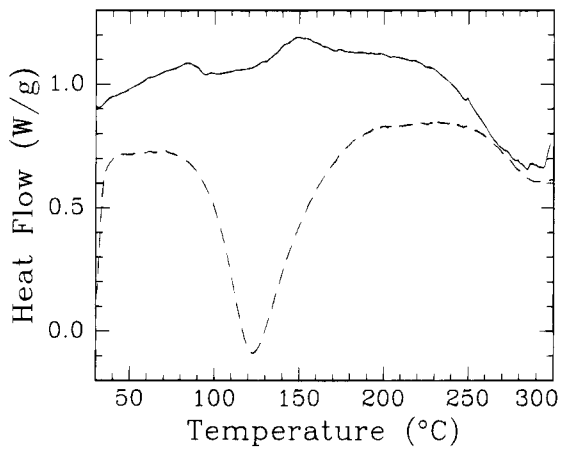

Figure 9. DSC curing scans of OMTS/DGEBA/BDMA (dashed line) and DGEBA/BDMA (solid line). DGEBA/BDMA sample was found to be uncured following rapid cooling to room temperature.

opening to build up the cross-linked epoxy network. It is interesting to note that the temparature at which curing occurs (approximately 100 °C as shown by the exotherm in Figure 9) corresponds to the same temperature that delamination of OMTS occurred (see Figure 4). The temperature coincidence of curing and delamination makes intuitive sense, since delamination exposes the hydroxyl groups of the alkylammonium chains in the interlayer to DGEBA and BDMA.

The participation of the hydroxylated OMTS alkylammonium ion in the curing reaction is more clearly illustrated with the OMTS/DGEBA/NMA system. Interestingly, full curing of the DGEBA/NMA mixture did not occur in the absence of OMTS, regrdless of heating

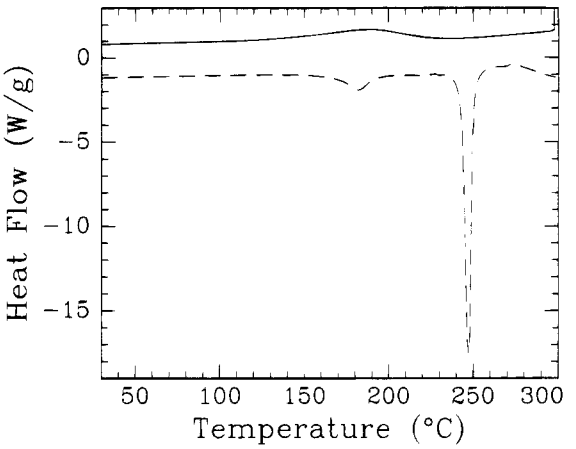

Figure 10. DSC curing scans of OMTS/DGEBA/NMA (dashed line) and DGEBA/NMA (solid line). DGEBA/NMA sample was found to be uncured following rapid cooling to room temperature.

rate. Shown in Figure 10 are DSC scans of the OMTS/DGEBA/NMA curing reaction. During dynamic curing of this formulation two distinct exotherms are observed; a weak one at 180 °C followed by a strong exotherm at 247 °C. Although the complete sequence of reactions has not yet been determined, a possible sequence might first involve the reaction of OMTS hydroxyl groups with NMA to form the monoester, **II**, as shown in eq 3.[39,41]

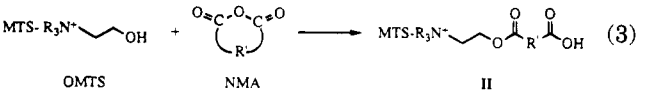

(3)

Nascent carboxylic groups of **II** can subsequently react with the epoxide resulting in formation of the diester, **III,** according to eq 4. Further reaction of **III** with

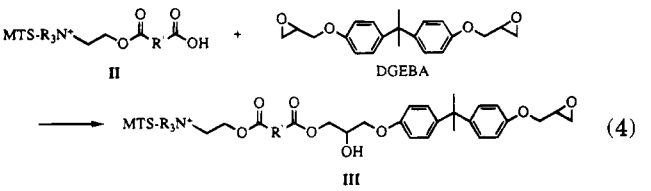

(4)

DGEBA results in epoxy network formation. This reaction sequence results in chemical bonding between the OMTS and the epoxy network. Although further work is required to verify the reaction pathway involved, it is clear from the data shown in Figure 10 that in the absence of OMTS, the DGEBA/NMA formulation does not result in curing under the conditions used in this experiment. This provides further evidence that the organic component of the OMTS participates in the curing reaction.

Mechanical Properties of the Nanocomposite. The effect of molecular dispersion of the silicate layers on the viscoelastic properties of the cross-linked polymeric matrix was probed using DMA. This experiment involves applying an oscillatory strain to a sample while monitoring the resultant stress, which consists of both in-phase and out-of-phase components.[44] These stresses can then be used to calculate the in-phase (E') and out-of-phase (E'') components of the modulus. The ratio E''/

(44) Ferry, J. D. *Viscoelastic Properties of Polymers*; John Wiley: New York, 1980.

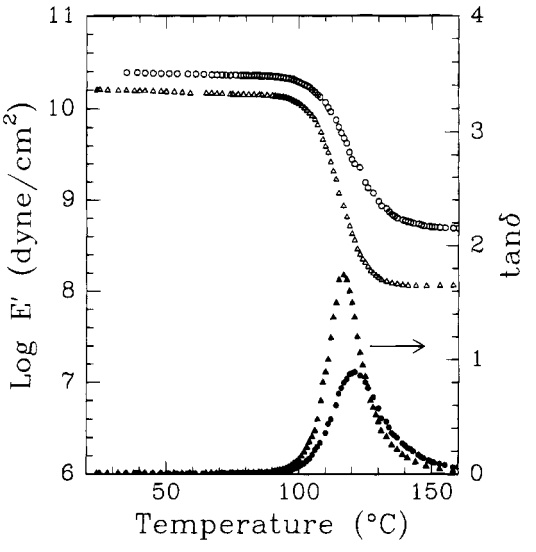

Figure 11. Temperature dependence of E' (open symbols) and tan δ (shaded symbols) for fully cured DGEBA/BDMA (△, ▲) and OMTS/DGEBA/BDMA (○, ●) containing 4% MTS by volume.

E' = tan δ is a measure of the ratio of energy lost to energy stored per cycle of deformation and typically goes through a maximum at the glass transition (T_g) of the polymer. At T_g there is a substantial drop in E', with a peak in tan δ indicating viscous damping due to segmental motion in the polymer.[44] For cross-linked polymers, both E' and T_g generally increase with cross-link density.

Shown in Figure 11 are the temperature dependencies of the tensile storage modulus, E', and tan δ of the OMTS/DGEBA/BDMA composite containing 4% silicate by volume[43] and the DGEBA/BDMA epoxy without any silicate. The shift and broadening of the tan δ peak to higher temperatures indicates an increase in nanocomposite T_g and broadening of the glass transition. The shift in T_g as measured by the tan δ peak maximum is on the order of only a few degrees (4 °C for the sample shown in Figure 11) and cannot account for the significant increase in plateau modulus. Furthermore, since the extent of curing is comparable in both samples (as measured by DSC), the increase cannot be attributed to variations in curing. Broadening and increase of T_g have been observed in other organic–inorganic nanocomposites and are generally attributed to restricted segmental motions near the organic–inorganic interface.[45-47] Chemical bonding at the interface of the silicate and epoxy matrix could lead to hindered relaxational mobility in the polymer segments near the interface, which leads to broadening and increase of T_g.

Below T_g, both samples exhibit high storage modulus, with a slight decrease in E' with increasing temperature. Notably, E' in the glassy region below T_g is approximately 58% higher in the nanocomposite compared to the pure epoxy (2.44×10^{10} compared to 1.55×10^{10} dyne/cm^2 at 40 °C). Even more striking is the large increase in E' at the rubbery plateau of the nanocomposite as shown in Figure 11. The nanocomposite exhibits a plateau modulus approximately 4.5 times higher than the unmodified epoxy (5.0×10^8 compared to 1.1×10^8 dyn/cm^2 at 150 °C). These changes are considerable, particularly in view of the fact that the silicate content is only 4% by volume. In this context, it is interesting to compare these results with reports of viscoelastic properties of conventionally prepared epoxy composites containing micron or larger size filler particles. Typically, the conventional filled epoxies do not exhibit substantial changes in E' at the filler volume contents (<10%) used in this study.[26-28]

Theoretical expressions have been derived by Halpin and Tsai[48] to calculate elastic modulus of a composite consisting of uniaxially oriented particles of filler suspended in a continuous matrix. For composites with platelike particles, these equations predict a strong dependence of composite elastic modulus on filler aspect ratio.[49] Solving the simultaneous Halpin–Tsai equations with the experimental dynamic storage modulus data in the glassy and the rubbery region yielded an apparent aspect ratio of 43. It is clear from the TEM micrographs shown in Figure 7 that some relatively unmodified epoxy matrix exists between the domains of 5–10 delaminated silicate layers. As a result, the effective aspect ratio of the silicate-rich domains could be much lower than the 100–1000 predicted for fully delaminated and dispersed silicate layers. More detailed experiments on nanocomposites containing a range of filler contents and particle sizes are underway to establish the full relationships between silicate content, aspect ratio, and composite properties.

Conclusions

Polymer–ceramic nanocomposites consisting of individual mica-type silicate layers embedded within a cross-linked epoxy matrix have been prepared. The synthetic approach involves delamination of OMTS within an epoxy resin, followed by curing of the crosslinked network. Separation of adjacent silicate layers by 100 Å or more was verified by XRD and TEM analysis, with good wetting of the silicate surface by the epoxy matrix. Dynamic mechanical analysis of the nanocomposite showed significant increases in dynamic storage modulus when only small amounts (4% by volume) of silicate were added, along with a broadening and slight increase in T_g. The glass transition broadening effect could be due to good interfacial adhesion between the epoxy matrix and silicate particles or to a restriction of molecular mobility of polymeric segments near the silicate surface. The nanocomposite exhibits dynamic modulus reinforcement greater than conventionally filled epoxies with comparable filler loadings, and may lead to improved, lightweight epoxy composites for application as adhesives, coatings, electronic, or structural materials.

Acknowledgment. The authors would like to acknowledge the financial support of the AFOSR, Southern Clay Corp., and Corning, Inc. We benefited from the use of MRL Central Facilities funded by the National Science Foundation. We thank C. K. Ober for useful discussions and advice, and we thank J. Chisaki for assistance with TEM imaging.

(45) Landry, C. J. T.; et al. *Macromolecules* **1993**, *26*, 3702.
(46) Huang, H.-H.; Wilkes, G. L.; Carlson, J. G. *Polymer* **1989**, *30*, 2001.
(47) Huang, H.-H.; Orler, B.; Wilkes, G. L. *Macromolecules* **1987**, *20*, 1322.
(48) Halpin, J. C.; Kardos, J. L. *Polym. Eng. Sci.* **1976**, *16*, 344.
(49) Rexer, J.; Anderson, E. *Polym. Eng. Sci.* **1979**, *19*, 1.